Fabrication of YAG/Cr:YAG transparent composite ceramics and characterization by light sheet fluorescence imaging

Lucie Chretien, Rémy Boulesteix, Fabien Bouzat, Camille Perrière, Alexandre Maitre, Christian Sallé, Alain Brenier, Yannick Guyot

Fabrication of YAG/Cr:YAG transparent composite ceramics and characterization by light sheet fluorescence imaging

Rémy Boulesteix[1,2*], Fabien Bouzat[1,2], Camille Perrière[1,2], Alexandre Maître[1,2], Christian Sallé[2,3], Alain Brenier[4], Yannick Guyot[4]

[1] Univ. Limoges, IRCER, UMR CNRS 7315, F-87068 Limoges, FRANCE

[2] LCTL, IRCER, UMR CNRS 7315, F-87068 Limoges, FRANCE

[3] CILAS, F-45063 Orléans, FRANCE

[4] Univ. Claude Bernard Lyon 1, ILM, UMR CNRS 5306, F-69622 Lyon, FRANCE

(*) Author to whom the correspondence should be addressed

Tel.: +33 (0)5 87 50 23 45 Fax: +33 (0)5 87 50 23 04 E-mail: remy.boulesteix@unilim.fr

Abstract

Transparent composite ceramics based on YAG/Cr:YAG bilayer samples were manufactured by the solid-state reaction route and sequential slip-casting technique. They were characterised by light sheet fluorescence imaging (LSFI). This work shows that LSFI allows determining the spatial distribution of chromium with different valence state (Cr^{4+} and Cr^{3+}) with a resolution close to 5 µm and high sensitivity in regards to the concentration. LSFI thus appears well adapted to the characterisation of transparent ceramic materials with luminescent dopant gradient used as solid-state lasers optical components.

Keywords:

YAG:Cr^{4+}, transparent ceramics ; LSFI ; saturable absorber

1. Introduction

Yttrium Aluminum Garnet (YAG, $Y_3Al_5O_{12}$) is an excellent host for high power solid-state lasers due to its good mechanical and optical properties [1]. This matrix allows incorporation in solid solution of luminescent ions such as rare-earth elements (*e.g.* Nd^{3+}, Yb^{3+}, Ho^{3+}) or transition metals

(*e.g.* Cr^{3+}, Cr^{4+}). Among them, chromium +IV-doped Yttrium Aluminum Garnet (Cr^{4+}:YAG) can be used as a saturable absorber of pulsed lasers emitting around 1 µm because it has a strong absorption band with a short de-excitation lifetime at this wavelength. The flexibility of ceramic processes also allow developing optical components with new architectures, *i.e.* concentration gradient of luminescent dopants. As a result, optical components with multilayers, clad-core or continuous gradient can be envisaged [1,2]. Nevertheless, the characterization of dopant distribution in the final components remains an issue, as common techniques are destructive. Moreover, the majority of them (SEM-EDXS, electron microprobe, SIMS, etc.) present detection limit too high to quantify dopant concentration and/or are non-sensitive to the valence of ions. For the development of optical components with complex architecture, for example with non-planar dopant concentration gradient and/or multi-dopant gradient, new characterizations techniques are thus needed.

Light sheet Fluorescence Microscopy (LSFM) is a non-destructive characterization technique extensively used in cell-biology for imaging within whole organisms [3] and allowing 3-dimensional reconstruction. Due to the excitation with a thin plane of light it has the advantage of fast acquisition and weak perturbation of the sample [4]. The gentle light excitation allows in vivo imaging over long periods of time [5]. Combined with an arrangement providing an extended depth of field, a large volumetric field of view can be explored at high speed [6].

This work was focused on the implementation of Light Sheet Fluorescence Imaging (LSFI) technique to characterise the distribution of chromium in two-layers YAG/Cr:YAG: transparent composite ceramics. First, the manufacturing process of such samples was detailed in this paper. It is based on the well-known solid-state reaction sintering process coupled with sequential slip-casting process. Surface polished transparent ceramics were then characterised by LSFI.

2. Methods

2.1. Samples preparation

YAG/Cr^{4+}:YAG transparent composite ceramics were elaborated by a solid-state reactive sintering process. In this process, pure oxides were mixed together, shaped in the form of pellets and then reaction-sintered at high temperature. In this study, Si^{4+} was used as sintering aid in pure YAG matrix whereas Ca^{2+} and Mg^{2+} cations were used as sintering aid and charge compensators to stabilise the valence +IV of chromium ions in Cr:YAG matrix. Commercial submicron ±-Al_2O_3 (Ø < 0.5 µm; purity > 99.99 %, Baïkowski, France), Y_2O_3 (Ø < 0.5 µm; purity > 99.99 %, AMPERE Industry, France), SiO_2, MgO, $CaCO_3$ and Cr_2O_3 (Ø < 1 µm; purity > 99.99 %, Alfa Aesar, Germany) were blended together in deionized water and ball-milled with corundum balls in order to obtain homogeneous slurries. Pellets of 10 mm in diameter with two layers each of 10 mm in thickness (one first layer of YAG:Cr then a second layer of undoped YAG) were shaped by sequential slip casting as described

elsewhere [7]. Dried samples were calcined under air at T < 1173 K to remove organic residues. Reaction-sintering was conducted under vacuum in a tungsten mesh-heated furnace (P d 10^{-3} Pa) at 1993 K for 10 h. Green bodies were placed in alumina crucible with heating and cooling rates of 5 $K.min^{-1}$. Samples were finally annealed under air at 1023 K for 10 h to change the valence +III to +IV of chromium ions.

2.2. Characterisations

After sintering, the crystalline phases were identified and indexed by X-ray diffraction analysis (D8, Bruker, Karlsruhe, Germany) using Cu $K_{\pm1}$ main radiation. Indexation of crystalline phases was carried out by the DIFFRAC^{plus} EVA^{TM} software and the PDFmain^{TM} database. Diffraction intensity owing to Cu $K_{\pm2}$ radiation with lower intensity was removed from obtained diagrams by EVA^{TM} software. Sintered samples were then polished with 1 µm diamond paste and thermally etched under air at 100 K below the sintering temperature to investigate their microstructure by scanning electron microscopy (FEG-SEM Quanta 450, FEI, Thermo Fisher Scientific, USA).

Transmittance optical measurements were realised with UV-visible spectrophotometer Cary 5000 (Varian, USA). The Cr^{4+} emission spectra were recorded under CW 970nm-LED excitation with the help of a InGaAs iDUS CCD camera following an ANDOR Technology Shamrock500i monochromator (300 l/mm grating blazed at 1000 nm). The luminescence decay curves were recorded under pulsed laser excitation (OPO laser, EKSPLA NT342, 10Hz repetition rate, 7ns pulse duration), the fluorescence being detected with a Hamamatsu NIR PMT H10330B-75 through the same monochromator and coupled to a Waverunner 64Xi digital scope.

The distribution of the Cr^{3+} and Cr^{4+} ions near the interface separating the Cr-doped YAG and the undoped YAG of the composite samples was visualised by LSFI. In this technique (see Figure 1), the Cr fluorescence is excited from a laser and is imaged on a camera through the face perpendicular to the beam. The laser beam, having a M^2 quality factor close to 1, is first shaped as a vertical thin sheet illuminating only the part of the sample to be observed. This contributes to reduce the background as in confocal microscopy but with a much higher acquisition speed. The sheet is obtained thanks to three cylindrical lenses L_1, L_2 and L_3 and a doublet L_4. An actuator allows moving the sample perpendicularly to the light sheet in order to explore different planes. An observed detail corresponds to a thickness resolution which is the sheet thickness measured to be 130 µm over a length given by the confocal parameter, calculated to be about 20 cm, which is much larger than the expected details inside the sample. The light sheet fluorescence was imaged on the camera with lenses (a lone lens in shown in Figure 1 for simplification) with different magnifications but we mainly used 1:1 imaging in this work (no magnification).

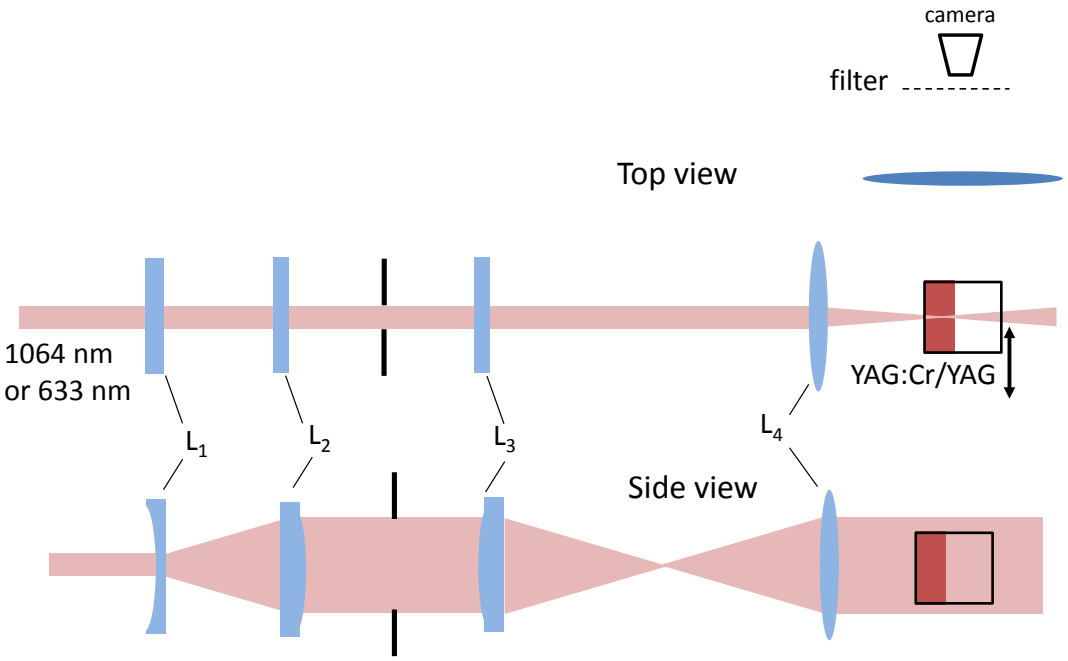

Figure 1: Scheme of light sheet fluorescence imaging used for composite ceramics characterisation.

The octahedral site Cr^{3+} fluorescence was selected close to the maximum intensity of the $^4T_2 \rightarrow {}^4A_2$ transition with a 700 nm interference filter (10 nm FWHM). It was detected by a Beamage Focus II CCD camera from Gentec. The number of pixels was 1360 x 1024 and the pixel size was 15 µm. The excitation was provided by a Helium-Neon laser at 632.8 nm.

The tetrahedral site Cr^{4+} fluorescence was selected close to the maximum intensity of the $^3T_2 \rightarrow {}^3A_2$ transition with a 1400 nm interference filter (10 nm FWHM). It was detected by a Xeva 1.7-640 InGaAs camera from Xenics, cooled down to 263 K by a Pelletier thermoelectric cooler. The number of pixels was 640 x 512 and the pixel size was 20 µm. The excitation was provided by a 1064 nm Nd:YAG laser.

3. Results and discussion

3.1. Structural and microstructural analyses

Samples were first characterised by SEM (Figure 2). The two regions were transparent with dense and homogeneous microstructure. No secondary phases, impurities or pores were observed in both regions. Nevertheless, grains diameter appears drastically different between the two regions: 12.5 µm for the undoped region and 1.47 µm for Cr-doped region. This difference can be related to the different sintering aids used to obtain transparent YAG and Cr:YAG ceramics: Si^{4+} was used for undoped YAG and Ca^{2+} and Mg^{2+} were used for Cr-doped YAG region. It is well known that silicon is a very efficient sintering aid in YAG that strongly promotes densification but also grain growth [8,9].

On the other hand, Ca and Mg as sintering aids tend to limit grain growth [10]. As a result, fully dense and transparent YAG ceramics were obtained in both cases but with different microstructures.

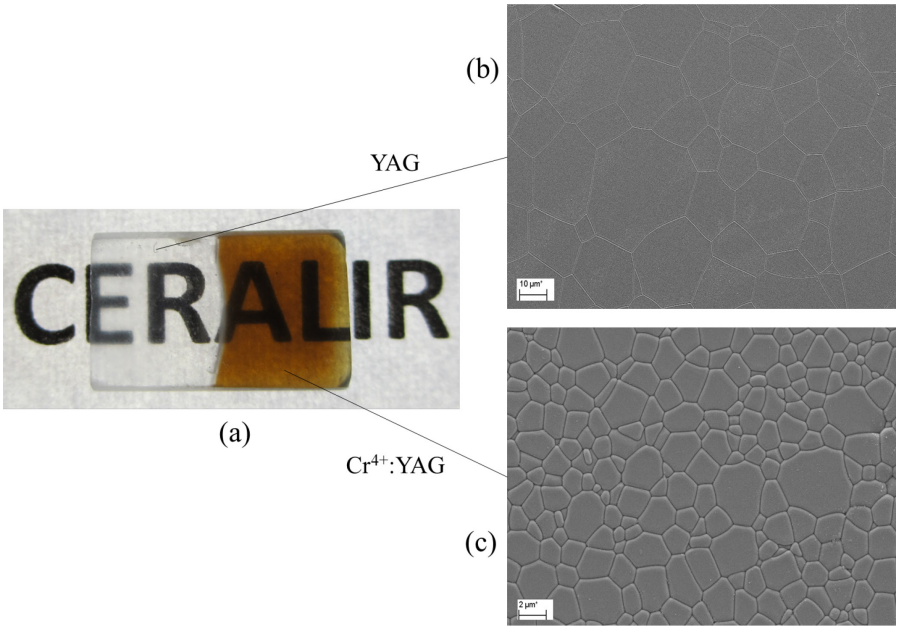

Figure 2: (a) Picture of transparent YAG/Cr^{4+}:YAG transparent ceramic sample and corresponding SEM micrographs: (b) undoped region and (c) Cr-doped region.

Chromium can have different valence state (essentially +III and +IV in YAG) and thus different size (0.062 nm and 0.055 nm, respectively [11,12]). As a consequence, Cr^{3+} tends to enter in solid solution on octahedral Al^{3+} site, whereas smaller Cr^{4+} tends to substitute Al^{3+} in tetrahedral site. In general, manufacturing of YAG:Cr^{4+} single-crystals by Czochralski method reports the necessity to use divalent Ca^{2+} ions as co-dopant. Prolonged heating at high temperature in air transforms a fraction of Cr^{3+} into Cr^{4+} whereas a reducing atmosphere provides a full reduction into Cr^{3+} [13,14]. Moreover, the diffusion of oxygen vacancies was established while the oxidation processes can be followed by absorption and fluorescence characteristics. Consequently, chromium remains in valence state +III after growing and supplementary annealing under oxidizing atmosphere is necessary to change its valence to +IV. These works also put in evidence that introduction in YAG of cations of valence +II (like Ca^{2+} and/or Mg^{2+}) is necessary to act as charge compensator thus allowing the change of chromium oxidation state to +III to +IV. In regards to their size, Ca^{2+} with diameter of 0,112 nm substitute preferably Y^{3+} dodecahedral site whereas Mg^{2+} with diameter of 0,06 nm substitute preferably Al^{3+} octahedral site. As a result the general formulae obtained for homogeneous and totally substituted YAG:Cr ceramics is $Y_{3-x}Ca_xAl_{5-y-z}Mg_yCr_zO_{12}$. According to this formulae, YAG phase incorporating 0.1%at.Cr, 0.04%at.Mg and 0.16%at.Ca as used in this work should be written $Y_{2.9952}Ca_{0.0048}Al_{4.9937}Mg_{0.002}Cr_{0.005}O_{12}$.

Samples were then analysed by XRD (Figure 3). Obtained spectra show that samples are single-phased as all diffraction peaks correspond to YAG cubic phase (JCPDS file 00-033-040). As no secondary phases were detected by SEM and XRD, it can be supposed that all additional elements (Cr, Mg, Ca and Si) should totally enter in solid-solution in YAG matrix.

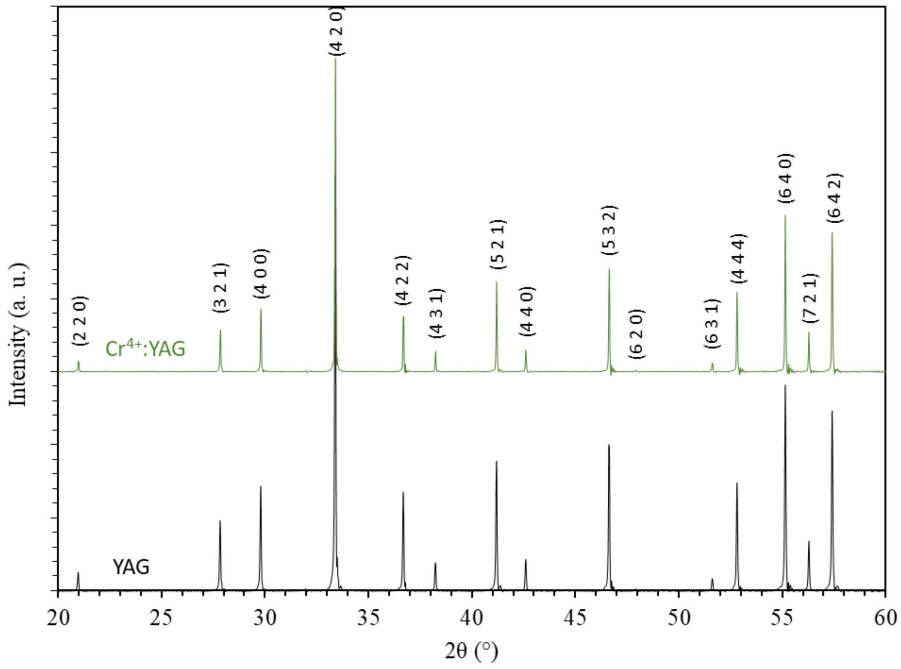

Figure 3: XRD analyses of undoped YAG and Cr^{4+}:YAG transparent ceramics.

Then, Cr^{4+}:YAG ceramics were characterised by UV-Vis-NIR spectrophotometry. The two absorption peaks near 430 and 600 nm in the Cr:YAG as-sintered ceramic in Fig. 4 are attributed respectively to the $^4A_2 \rightarrow {}^4T_1$ and $^4T_2$ transitions of Cr^{3+} in octahedral site. The main broad band appearing near 1 µm in the annealed ceramic is attributed to the $^3A_2 \rightarrow {}^3T_2$ transition of Cr^{4+} in tetrahedral site.

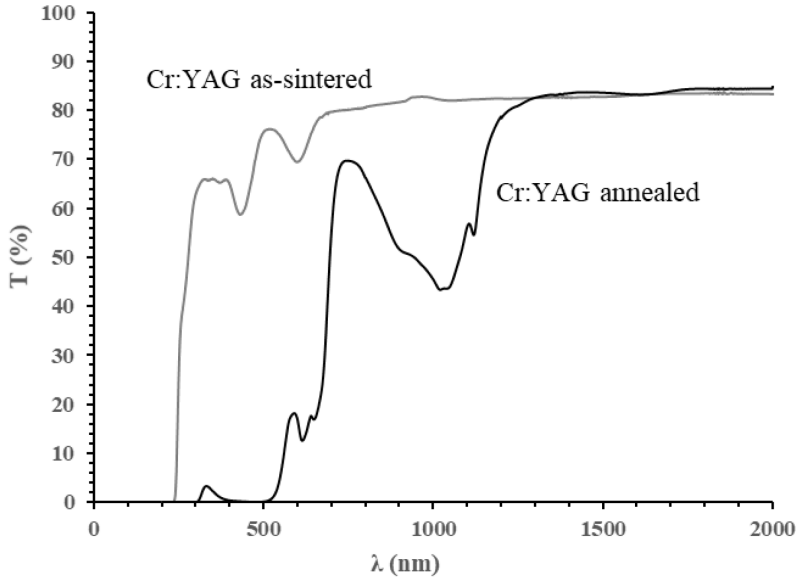

Figure 4: Transmittance spectra for as-sintered and air annealed (1023 K for 10 h) Cr:YAG ceramics specimens with 2.5 mm in thickness.

A typical Cr^{4+}-doped YAG emission spectrum shown in the Figure 5a extend from about 1150 nm up to 1600 nm with a maximum around 1350 nm corresponds to the broad band transition $^3B_2$ ($^3T_2$)→ $^3B_1$ ($^3A_2$) [15]. The presence of Cr^{3+} was evidenced by recording the emission spectrum around 700 nm when the annealed sample is excited in green domain [16]. The luminescence decay curve presented in Figure 5b is perfectly exponential showing a good homogeneity of the doping ions. The room temperature lifetime of 4.1 μs is similar than the value obtained by Kück [17].

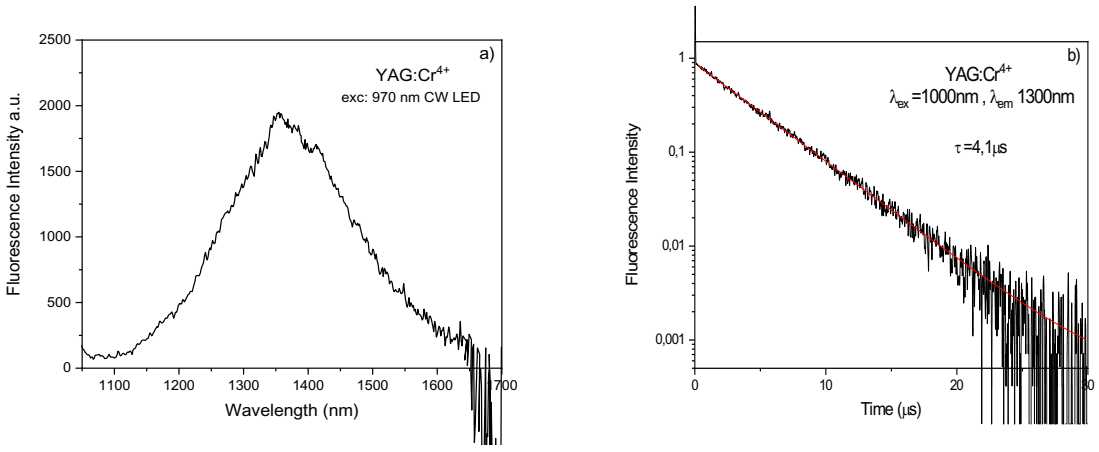

Figure 5: Emission spectrum (corrected from the response apparatus) of Cr^{4+}:YAG sample under 970 nm excitation (a) and corresponding lifetime under 1000 nm excitation and 1300 nm emission (b).

3.2. Cr^{4+} concentration analyses by light sheet fluorescence imaging

First, the Cr^{4+} concentration of a homogenous doped sample was deduced by the relation:

$$[Cr^{4+}] = \frac{k}{\sigma_a}$$

where k is the absorption coefficient at 1064 nm and $\sigma_a = 5.04\ 10^{-19}$ cm^2 is the Cr^{4+}:YAG absorption cross-section at 1064 nm. Obtained results show that Cr^{4+}/Cr_{total} concentration ratio is close to 66% in analysed ceramic samples, *i.e.* 66% of chromium ions are in the valence +IV and 34% in are in valence +III. Compared to results obtained on single-crystals [13], the conversion ratio of Cr^{3+} to Cr^{4+} is more efficient in YAG ceramics (50% and 66% respectively). This result could be explained by better charge compensation process in ceramics owing to higher solubility of Ca^{2+} and Mg^{2+} at the sintering temperature used for ceramics (*i.e.* 1993 K in this study) compared to melting temperatures commonly used for YAG single-crystal growth (*i.e.* 2223 K).

Transparent composite Cr:YAG ceramics were analysed by LSFI recorded at two wavelengths: (1) 1.4 µm for Cr^{4+} detection, *i.e.* at the maximum fluorescence intensity for this ion under excitation at 970 nm (see Figure 5a), and (2) 0.7 µm for Cr^{3+} detection, *i.e.* at the maximum fluorescence intensity for this ion under excitation at 532 nm. Results were presented in Figure 6. First, Figure 6a shows rough LSFI signal at 1.4 µm of a composite sample. The dotted line corresponds to the illumination plane. As expected, fluorescence (in red/yellow in Figure 6a) is only visible in the Cr^{4+} doped region (bottom of the image) whereas the undoped YAG region shows no fluorescence at 1.4 µm. Fluorescence is also visible close to the main signal and on the sample edge due to light scattering by residual defects and light reflection at the surface of sample. Second, Cr^{3+} and Cr^{4+} concentration profiles were plotted in Figure 6b. The shape of both signals is in accordance with the simple bilayer architecture of this composite. Transition region between undoped and doped region is clearly visible in Figure 6b at a position around 3800 µm that corresponds roughly to the center of the image in Figure 6a (*i.e.* middle position between A and B points). The transition is not very sharp that means some interdiffusion of chromium should occur during thermal treatments. Recorded diffusion length from initial interface in Figure 6b (around 180 µm for Cr^{3+} and 260 µm for Cr^{4+}) seems to show that Cr^{4+} diffuses more efficiently than Cr^{3+}. Such result must be confirmed with an improved resolution of our apparatus in the future.

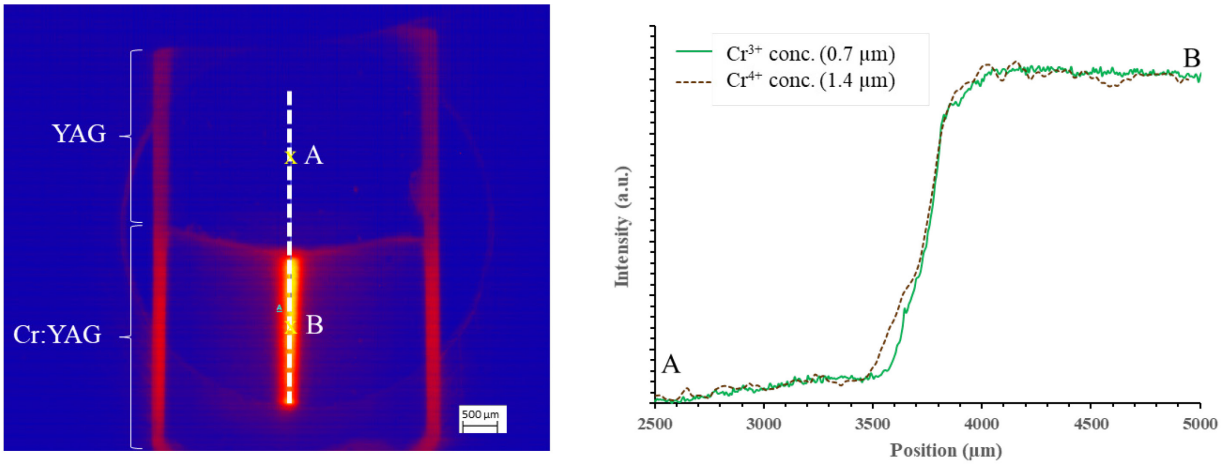

Figure 6: Light sheet Fluorescence image at 1.4 µm (Cr^{4+}) in annealed YAG/Cr:YAG specimen (collinear imaging mode) (a); Fluorescence intensity along the white line obtained at 0.7 µm and 1.4 µm for the determination of Cr^{3+} and Cr^{4+} concentration, respectively (b).

A second sample was characterised by LSFI in perpendicular imaging mode corresponding to the illustration in Figure 1. In this mode, a view of an internal slice of a YAG/Cr^{3+}:YAG composite ceramic was obtained and presented in Figure 7. In Figure 7b, undoped YAG region is visible because of some light scattering due to small amount of residual defects in the sample. Cr^{3+} doped region is also clearly visible. The difference in intensity signal in doped region is due to inhomogeneous intensity in the light sheet (Gaussian shape of intensity). This can be easily solved by software correction and/or some improvements of the optical system should be carried out to limit this phenomenon.

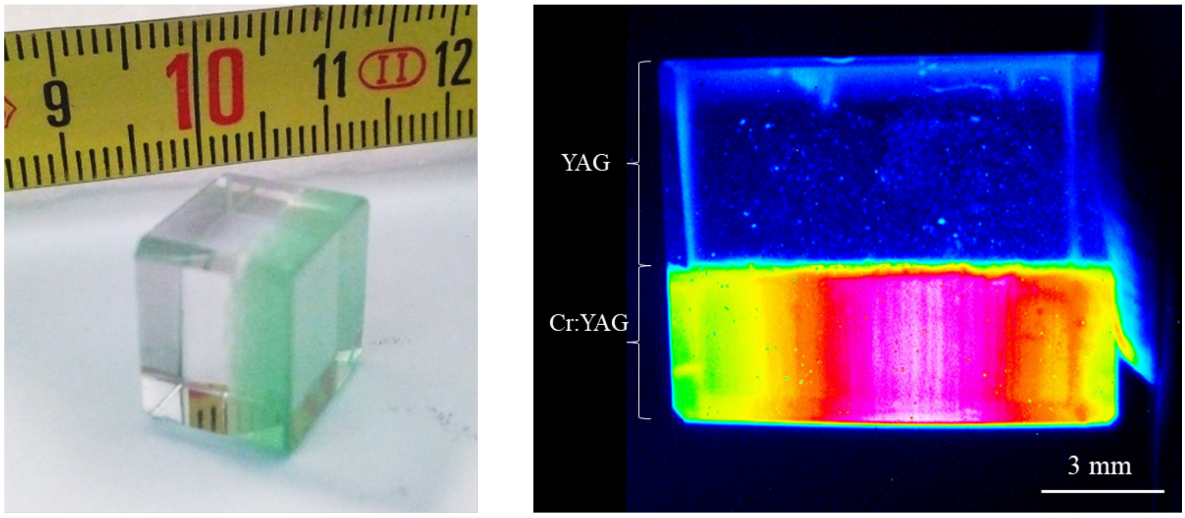

(a) (b)

Figure 7: View of YAG/Cr^{3+}:YAG specimen (a) and corresponding LSFI at 0.7 µm in perpendicular imaging mode (b).

Conclusions

To conclude, this study allows to draw some conclusions. Fully dense YAG/YAG:Cr (Cr +III or +IV) composite ceramics can be manufactured by sequential slip-casting and reactive sintering technique. Then, Light Sheet Fluorescence Imaging (LSFI) appears to be a well adapted and non-destructive technique to determine dopant concentration and distribution in composite transparent ceramics. Further work will be conducted in order to better manage optical aberration and imaging resolution.

Acknowledgments

This work is a part of the CERALIR project. We would like to thank the ANR (French National Research Agency) for its support and DGA (French armaments procurement agency) for funding under grant Nb.

Bibliography

[1] A. Ikesue, Y.L. Aung, Ceramic laser materials, Nature Photonics. 2 (2008) 721–727. doi:10.1038/nphoton.2008.243.

[2] R. Belon, R. Boulesteix, P.M. Geffroy, A. Maitre, C. Sallé, T. Chartier, Tape casting of multilayer YAG-Nd:YAG transparent ceramics for laser applications: Study of green tapes properties, J. Eur. Ceram. Soc. 39 (2019) 2161–2167.
[3] P.A. Santi, Light Sheet Fluorescence Microscopy: A Review, Journal of Histochemistry & Cytochemistry. 59 (2001) 129–138.
[4] J.M. Heddleston, T.-L. Chew, Light sheet microscopes: Novel imaging toolbox for visualizing life's processes, The International Journal of Biochemistry & Cell Biology. 80 (2016) 119–123.
[5] G. de Medeiros, B. Balázs, Light-sheet imaging of mammalian development, Seminars in Cell & Developmental Biology. 55 (2016) 148–155.
[6] R. Tomer, M. Lovett-Barron, I. Kauvar, A. Andalman, V.M. Burns, S. Sankaran, L. Grosenick, M. Broxton, S. Yang, K. Deisseroth, SPED Light Sheet Microscopy: Fast Mapping of Biological System Structure and Function, Cell. 163 (2015) 1796–1806.
[7] L. Bonnet, R. Boulesteix, A. Maître, C. Sallé, V. Couderc, A. Brenier, Manufacturing issues and optical properties of rare-earth (Y, Lu, Sc, Nd) aluminate garnets composite transparent ceramics, Optical Materials. 50 (2015) 2–10. doi:10.1016/j.optmat.2015.04.050.
[8] R. Boulesteix, A. Maître, J.-F. Baumard, Y. Rabinovitch, C. Sallé, S. Weber, M. Kilo, The effect of silica doping on neodymium diffusion in yttrium aluminum garnet ceramics: implications for sintering mechanisms, J. Eur. Ceram. Soc. 29 (2009) 2517–2526.
[9] A.J. Stevenson, X. Li, M.A. Martinez, J.M. Anderson, D.L. Suchy, E.R. Kupp, E.C. Dickey, K.T. Mueller, G.L. Messing, Effect of SiO2 on Densification and Microstructure Development in Nd:YAG Transparent Ceramics, J. Am. Ceram. Soc. 94 (2011) 1380–1387.
[10] B. Wang, Q.X. Cao, Effect of MgO on the Microstructure of Polycrystalline Nd:YAG Ceramics and its Action Mechanism, Advanced Materials Research. 535–537 (2012) 836–839. doi:10.4028/www.scientific.net/AMR.535-537.836.
[11] R.D. Shannon, C.T. Prewitt, Effective Ionic Radii in Oxides and Fluorides, Acta Crystallogr., Sect. B: Struct. Sci. (1969) 925–946.
[12] K. Li, D. Xue, Estimation of Electronegativity Values of Elements in Different Valence States, J. Phys. Chem. A. 110 (2006) 11332–11337. doi:10.1021/jp062886k.
[13] A. Sugimoto, Y. Nobe, K. Yamagishi, Crystal growth and optical characterization of Cr,Ca: Y3Al5O12, Journal of Crystal Growth. 140 (1994) 349–354. doi:10.1016/0022-0248(94)90309-3.
[14] R. Feldman, Y. Shimony, Z. Burshtein, Dynamics of chromium ion valence transformations in Cr,Ca:YAG crystals used as laser gain and passive Q-switching media, Optical Materials. 24 (2003) 333–344. doi:10.1016/S0925-3467(03)00146-0.
[15] H. Eilers, U. Hömmerich, S.M. Jacobsen, W.M. Yen, K.R. Hoffman, W. Jia, Spectroscopy and dynamics of Cr4+:Y3Al5O12, Phys. Rev. B. 49 (1994) 15505–15513. doi:10.1103/PhysRevB.49.15505.
[16] K.M. Kinsman, J. McKittrick, E. Sluzky, K. Hesse, Phase development and luminescence in chromium-doped yttrium aluminum garnet (YAG:Cr) phosphors, Journal of the American Ceramic Society. 77 (1994) 2866–2872.
[17] S. Kück, K. Petermann, U. Pohlmann, G. Huber, Near-infrared emission of Cr4+-doped garnets: Lifetimes, quantum efficiencies, and emission cross sections, Phys. Rev. B. 51 (1995) 17323–17331. doi:10.1103/PhysRevB.51.17323.